Asymmetric simple exclusion process with position-dependent hopping rates: Phase diagram from boundary-layer analysis

Sutapa Mukherji
Department of Protein Chemistry and Technology, CSIR-Central Food Technological Research Institute, Mysore-570 020, India

(Received 6 September 2017; published 26 March 2018)

In this paper, we study a one-dimensional totally asymmetric simple exclusion process with position-dependent hopping rates. Under open boundary conditions, this system exhibits boundary-induced phase transitions in the steady state. Similarly to totally asymmetric simple exclusion processes with uniform hopping, the phase diagram consists of low-density, high-density, and maximal-current phases. In various phases, the shape of the average particle density profile across the lattice including its boundary-layer parts changes significantly. Using the tools of boundary-layer analysis, we obtain explicit solutions for the density profile in different phases. A detailed analysis of these solutions under different boundary conditions helps us obtain the equations for various phase boundaries. Next, we show how the shape of the entire density profile including the location of the boundary layers can be predicted from the fixed points of the differential equation describing the boundary layers. We discuss this in detail through several examples of density profiles in various phases. The maximal-current phase appears to be an especially interesting phase where the boundary layer flows to a bifurcation point on the fixed-point diagram.

DOI: 10.1103/PhysRevE.97.032130

I. INTRODUCTION

Totally asymmetric simple exclusion processes (TASEPs) are driven many-particle systems in which particles hop unidirectionally along a one-dimensional lattice obeying exclusion principle [1]. The exclusion principle rules out double occupancy and hence a hopping is possible if the target site is empty. In a system with open boundaries, particles are injected into the lattice through one boundary at a given rate. After injection, these particles hop towards the other boundary from which they are withdrawn at a given rate. In the steady state such systems are known to exhibit boundary induced phase transitions as the particle injection and withdrawal rates at the boundary are changed [2,3]. In different phases, the average density of particles across the lattice are significantly different and one of the important tasks in this context is to find out the shape of the average density profile across the lattice and characterize the phase transitions by studying the nature of the steady-state particle current or the shape of the density profile. The presence of such phase transitions is a speciality of such nonequilibrium systems and no equilibrium counterpart of this can be seen in one-dimensional equilibrium systems with short-range interactions. This has been the reason for extensive research in this area that has led to developments of new methods and introduction of new models [4–10], some of which have close resemblance with biological transport processes [11–14].

In the present paper, we consider a TASEP with open boundaries and with position-dependent hopping rates. In general, TASEPs with variable hopping rates are found to exhibit interesting dynamics [15–17]. Many of these models are motivated from intracellular transport processes which primarily involve motion of motor proteins on biopolymers such as microtubules, actin filaments, etc. [18]. In the present work, we consider the hopping rate to be linearly increasing with the position of the particle. The motivation for such a choice has connection to some of the recent experiments on biopolymers. Biopolymers such as microtubules are known to have their own polymerization-depolymerization dynamics due to which the length of the microtubule becomes a dynamically variable quantity. The polymerization dynamics of microtubules is found to be regulated by motor proteins functioning as polymerases or depolymerases [19]. These motor molecules move towards the tip of the microtubule and stabilize or destabilize the biopolymer on reaching the tip. Recent experiments reveal that many such regulation processes depend on the length of the microtubule [20–23]. It is believed that the motor proteins near the microtubule tip experience a "push" due to the motor proteins accumulated behind it [24]. As the length of the biopolymer increases, the number of motor proteins landing on it increases. As a consequence, the "push" generated by such motor molecules acquires a dependence on the length of the microtubule. Additionally, some of the recent experiments also predict that such destabilizing activity triggered by the "push" due to motor proteins accumulated behind depends linearly on the length of the microtubule [24]. In view of such observations, we assume that the hopping rate of a particle or a motor protein in a given position is influenced in a similar way by the number of particles behind it. Since the number of trailing particles behind a specific particle depends on its location along the lattice, we assume position-dependent hopping rates for the particles. As a result, the farther the particle is from the origin of the lattice, the larger its hopping rate. In addition, following the earlier predictions, we consider the hopping rate to be linearly dependent on the position of the particle.

TASEP and partially asymmetric simple exclusion processes with position-dependent hopping rates have been studied earlier using the mean-field approximation [15–17]. In Ref. [15], TASEP with hopping rate increasing linearly with

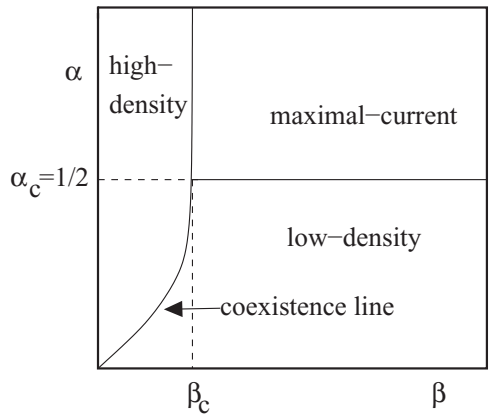

FIG. 1. Qualitative plot of the phase diagram. The solid lines represent the phase boundaries.

the position of the particle was studied for both periodic and open boundary conditions. In this case, the steady-state density profile with periodic boundary condition is found to have monotonically decreasing parts described through tan x-type function and also increasing kink like parts described through tanh x-type function, with x as the location along the lattice. These conclusions have strong connections with earlier studies on TASEP with uniform hopping rate and also with quenched random-bond case where the shape of the density profile depends crucially on whether the current density is greater or less than a critical value [25–27]. In case of open boundaries, TASEP with linearly increasing hopping rate shows boundary induced phase transitions as the injection and withdrawal rates are changed at the boundaries [15]. The phase diagram of such an open system is similar to that of ASEP with uniform hopping rate although there are distinct differences in the shape of the phase boundaries and also in the shape of the density profiles in these two models. The phase diagram, shown in Fig. 1, contains low-density, high-density, and maximal-current phases. As in the case of uniform hopping, in the low- and high-density phases, the particle density across most of the lattice remains smaller or larger than $1/2$, respectively. These two phases are separated from each other through a coexistence line. On the coexistence line, the density profile has both low- and high-density regions separated through a shock like discontinuous jump. In the maximal-current phase, the density allows maximum hopping current across the lattice.

It can be shown that in the continuum limit, the average particle density profiles in TASEPs, in general, are described through singular differential equations. Such a singular equation arises as one considers a continuum limit of the discrete master equation that describes the time evolution of particle occupancy at different lattice sites. The differential equation derived in this manner is singular since the highest-order derivative term (in our case, a second-order derivative term) in the differential equation appears along with a small prefactor proportional to the lattice spacing. In order to have a solution for the density profile, this equation has to be solved along with two boundary conditions which depend on the particle injection and withdrawal rates at the boundaries. In the extreme limit, i.e., when the second-order derivative term is completely ignored, the resulting first-order differential equation cannot, in general, satisfy two boundary conditions. In such a scenario, the vanishing second-order term acts as a regularizing term. As a consequence of the singularity, the solutions of such differential equations have narrow boundary-layer parts whose width depends on the small prefactor. Since the location, slope, and height of the boundary layers vary significantly in various phases, there have been attempts to understand the phase transitions by studying various properties of boundary layers under different boundary conditions [28,29].

The aim of the present paper is to show how the steady-state density profile of TASEP with position-dependent hopping rate and open boundaries can be obtained by solving directly the differential equation for the average particle density using the method of boundary-layer analysis. A careful analysis of this solution under different boundary conditions helps us obtain the phase boundaries associated with various boundary-induced phase transitions. In particular, we show that the coexistence line arises due to the deconfinement of the boundary layer from the boundary [28]. Although the phases in the phase diagram are similar to that of the ASEP with a uniform hopping rate, the average particle distribution across the lattice is significantly different from the uniform hopping case. Next, we obtain the fixed points (critical points) of the differential equation describing the boundary layers and show the stability properties of these fixed points on a phase portrait. Since the boundary-layer solution must be consistent with the flow pattern towards or away from a fixed point, the shape of the rest of the profile must also be appropriate to support such boundary layers and also, at the same time, satisfy the boundary conditions. Exploiting these conditions, it is possible to predict the shape of the entire density profile under different boundary conditions. Since this analysis is based on the fixed points of the boundary-layer equation, this prediction is possible even in the absence of any explicit solution for the boundary layer. We explain this for the present problem by considering possible density profiles in different phases. In this formulation, the maximal-current phase turns out to be a particularly interesting phase where the boundary-layer solution flows to the bifurcation point on the phase portrait.

II. MODEL

On introducing the model through a discrete master equation, we obtain a continuum limit of this equation. The differential equation obtained in the continuum limit is analyzed using the method of boundary-layer analysis.

We consider a lattice with N sites and lattice spacing, a. In the discrete picture, the dynamics of the particle can be described in terms of a variable τ_i that denotes the particle occupancy of the ith site. This variable can have values $\tau_i =$ 1 or 0 if the ith site is occupied or empty, respectively. The time evolution of the variable τ_i can be expressed as

$$\frac{d\tau_i}{dt} = r_{i-1}\tau_{i-1}(1-\tau_i) - r_i\tau_i(1-\tau_{i+1}), \tag{1}$$

where the terms on the right-hand side of the equation arise from particle hopping to the empty neighboring site. Here r_is are the position-dependent hopping rates. After a statistical averaging of Eq. (1), we simplify the resulting equation using the mean-field approximation scheme under which

$\langle \tau_i \tau_j \rangle \approx \langle \tau_i \rangle \langle \tau_j \rangle$. Finally, a continuum limit is obtained by considering $N \to \infty$ and $a \to 0$ limits with Na remaining finite. For simplicity, we choose $Na = 1$ in the following. Introducing the average particle density as $\langle \tau_i \rangle = \rho(x,t)$ where $x(= ia)$ is the location along the lattice, we do Taylor expansions of $\rho(x \pm a)$ and $r(x-a)$ in small a. The resulting continuum mean-field equation in the steady state ($\frac{d\rho}{dt} = 0$) is

$$\frac{a}{2}\left[r(x)\frac{d^2\rho}{dx^2} + 2\frac{d\rho}{dx}\frac{dr}{dx} - 2\rho\frac{d\rho}{dx}\frac{dr}{dx}\right] + \left[2r(x)\rho\frac{d\rho}{dx} - r(x)\frac{d\rho}{dx} - \rho\frac{dr}{dx} + \rho^2\frac{dr}{dx}\right] = 0. \quad (2)$$

In the following, we shall be considering a linearly varying hopping rate as

$$r(x) = \theta\left(x - \frac{1}{2}\right) + 1/2, \quad (3)$$

where θ is a constant. Accordingly, while deriving Eq. (2), we have considered $\frac{d^2}{dx^2}r(x) = 0$. In general, the time-dependent dynamics of the system can be expressed in terms of the continuity equation

$$\frac{\partial \rho}{\partial t}(x,t) = -\frac{\partial J}{\partial x}, \quad (4)$$

where J represents the particle current density. It is straightforward to find that for the present model

$$J = -\frac{a}{2}\left[r(x)\frac{d\rho}{dx} + (\rho - \rho^2)\frac{dr}{dx}\right] + r(x)\rho(1-\rho), \quad (5)$$

where the last term in (5) indicates the hopping current and the terms in the square bracket reflect the interaction of particles with its neighbors; $\theta = 0$ corresponds to the case of uniform hopping. Another important case, with which the present analysis may be compared, is the particle-nonconserving TASEP with uniform hopping rate. In this case, the particle number is not conserved due to the possibility of particle adsorption or desorption to or from the lattice at given rates. This system will be referred to in the following as TASEP with Langmuir kinetics (TASEP-LK). In order to obtain the steady-state density profile, Eq. (2) has to be solved for $\rho(x)$ with the boundary conditions $\rho(x=0) = \alpha$ and $\rho(x=1) = 1 - \beta = \gamma$. Although α and β are usually used in literature as the injection and withdrawal rates at the boundary, respectively, here we use the same notation for the boundary densities.

III. BOUNDARY-LAYER ANALYSIS

Equation (2) is a singular equation since the second-order derivative term appears with the small prefactor a. The singularity arises from the fact that in the extreme limit, i.e., for $a = 0$, such equation reduces to a first-order equation which cannot, in general, satisfy two boundary conditions. Such singular equations are known to have solutions with boundary layers the width of which strongly depends on the small parameter, a.

In the first approximation, Eq. (2) can be solved for $a = 0$. Such solution is expected to describe the major part of the density profile. This wide, smoothly varying part of the density profile solution will be referred below as the outer or the bulk solution. Since this is a solution of a first-order equation, such a solution can satisfy at most one of the boundary conditions. To account for the other boundary condition, a boundary-layer part appears in the density profile. Apart from satisfying the other boundary condition, this boundary-layer part must also saturate to the bulk solution at its other end. This forms a typical scenario where the boundary layer appears near one of the boundaries of the system and the rest of the density profile is described by the outer solution which satisfies the other boundary condition (see, for example, Fig. 2). Since the boundary layer must satisfy two conditions—a boundary condition and a condition for saturation to the outer solution, the second-order derivative term of the differential equation (2) becomes important for the description of the boundary layer. There might be other scenarios where the boundary layer appears somewhere in the interior of the system and merges to two outer or bulk solution parts at the two ends. In this case, each outer solution satisfies one boundary condition and the boundary layer satisfies two saturation conditions at its two ends. Thus, the location of the boundary-layer part of the solution need not be restricted only near the boundary of the system [12,28]. The boundary-layer analysis discussed in the following is based on the determination of the boundary layer and bulk parts of the solution and subsequently an asymptotic matching of the two solutions to find the full density profile [30].

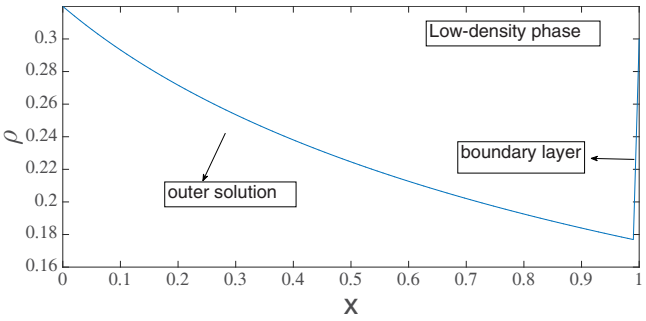

FIG. 2. A typical density profile in the low-density phase with a tanh-type boundary layer near $x = 1$ boundary. For this diagram, $\theta = 0.2$.

In order to find the outer solution, we substitute $a = 0$ in (2). The solution of the resulting first-order equation is

$$\rho_{\text{out},\pm}(x) = \tfrac{1}{2} \pm \tfrac{1}{2}\sqrt{1 + 4c/r(x)}, \quad (6)$$

where c is the integration constant. Note that two possible outer solutions are displayed in Eq. (6). The value of c can be determined from the boundary condition that the outer solution satisfies. For example, if this solution satisfies the boundary condition at $x = 0$, i.e., $\rho_{\text{out},\pm}(x=0) = \alpha$, then $c = \frac{\alpha(\alpha-1)(1-\theta)}{2}$. On the other hand, if the outer solution satisfies the boundary condition at $x = 1$, then $c = \frac{\beta(\beta-1)(1+\theta)}{2}$. With $\alpha, \beta < 1$, in general, c is negative in both cases for $\theta < 1$. Under these conditions, $\rho_{\text{out},+}$ and $\rho_{\text{out},-}$ have +ve and −ve slopes with x, respectively. Further, in accordance with Eq. (6), if an outer solution lies in the range $\rho > 1/2$, the outer solution is described by $\rho_{\text{out},+}$ and it has a positive slope with x. On the other hand, an outer solution with density value below $\frac{1}{2}$ is described by $\rho_{\text{out},-}$ which has a negative slope.

In order to find the boundary-layer part, it is convenient to introduce a rescaled variable $\tilde{x} = \frac{(x-x_0)}{a}$, where x_0 denotes the location of the boundary layer. For example, for a boundary layer appearing near the $x = 1$ boundary, $x_0 \approx 1$. Such a boundary layer must saturate to the outer solution for $x < 1$. Thus in the $a \to 0$ limit, such a saturation must happen as $\tilde{x} \to -\infty$. In terms of $\tilde{x}$, the differential equation, Eq. (2), is

$$\frac{1}{2a}\left[\frac{1}{2} + \theta(a\tilde{x} + x_0 - 1/2)\right]\frac{d^2\rho}{d\tilde{x}^2} + (1-\rho)\theta\frac{d\rho}{d\tilde{x}} + \frac{2\rho}{a}\left[\frac{1}{2} + \theta(a\tilde{x} + x_0 - 1/2)\right]\frac{d\rho}{d\tilde{x}} - \frac{1}{a}\left[\frac{1}{2} + \theta(a\tilde{x} + x_0 - 1/2)\right]\frac{d\rho}{d\tilde{x}} - \theta\rho + \theta\rho^2 = 0. \quad (7)$$

In the $a \to 0$ limit, we arrive at the boundary-layer equation

$$\frac{1}{2}\frac{d^2\rho}{d\tilde{x}^2} + 2\rho\frac{d\rho}{d\tilde{x}} - \frac{d\rho}{d\tilde{x}} = 0. \quad (8)$$

Possible solutions of this equation are

$$\rho_{\rm in}(\tilde{x}) = \frac{1}{2} + \frac{p}{2}\tanh[p(\tilde{x}+k)] \quad \text{and}$$
$$\rho_{\rm in}(\tilde{x}) = \frac{1}{2} + \frac{p}{2}\coth[p(\tilde{x}+k)], \quad (9)$$

where p and k are the integration constants whose values can be determined through the two conditions that the boundary-layer solutions must satisfy. For example, if the boundary layer appears near one boundary, (i) it must satisfy the boundary condition at that boundary, i.e., at $\tilde{x} = 0$, and (ii) the other end of the boundary layer must saturate to the bulk or the outer solution. Since, in the boundary layer language, this solution is often referred to as the inner solution, we have used subscript "in" in $\rho_{\rm in}$.

In the following, we consider different possibilities where the outer solution and the boundary-layer parts satisfy different conditions.

A. α-dominated phase or the low-density phase

In this case the outer solution satisfies the boundary condition at $x = 0$ and the boundary-layer solution accounts for the other boundary condition at $x = 1$. Hence,

$$2\alpha - 1 = \pm\sqrt{1 + 4c/r(x=0)}. \quad (10)$$

For such a phase, β should be above certain critical value derived in the next subsection. Further, as we shall show in Sec. IV, a density profile with the outer solution satisfying the boundary condition at $x = 0$ is possible provided $\alpha < \frac{1}{2}$. Hence, as per Eq. (6), for $\alpha < \frac{1}{2}$, the outer solution must be described by $\rho_{\rm out,-}$ with $c = \frac{1}{2}\alpha(\alpha-1)(1-\theta)$. A density profile of this kind has been displayed in Fig. 2. The boundary layer must saturate to the outer solution as $x \to 1-$(or $\tilde{x} \to -\infty$ since $x_0 \approx 1$). Thus

$$\rho_{\rm out,-}(x=1) = \frac{1}{2} - \frac{1}{2}\sqrt{1 + \frac{4\alpha(\alpha-1)(1-\theta)}{1+\theta}} = \rho_{\rm in}(\tilde{x} \to -\infty). \quad (11)$$

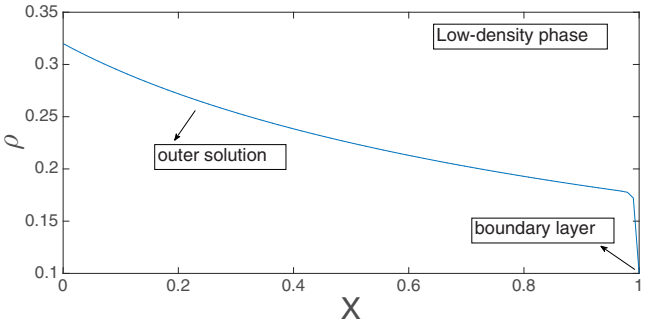

FIG. 3. A typical density profile in the low-density phase with a coth-type boundary layer near the $x = 1$ boundary. For this diagram, $\theta = 0.2$.

Two different types of boundary-layer solutions may appear near the $x = 1$ boundary.

(i) If $1 - \beta > \rho_{\rm out,-}(x = 1)$, then the boundary layer must have a positive slope to satisfy the boundary condition (as in Fig. 2). This is possible through a tanh-type boundary-layer solution which saturates to the outer solution if

$$\frac{1}{2} - \frac{p}{2} = \frac{1}{2} - \frac{1}{2}\sqrt{1 + \frac{4\alpha(\alpha-1)(1-\theta)}{1+\theta}}. \quad (12)$$

A boundary layer of tanh kind would satisfy the boundary condition at $x = 1$ ($\tilde{x} = 0$) if

$$\frac{1}{2} + \frac{p}{2}\tanh[pk] = 1 - \beta. \quad (13)$$

In the $\tilde{x} \to \infty$ limit, such a tanh-type solution saturates to

$$\frac{1}{2} + \frac{p}{2} = \frac{1}{2} + \frac{1}{2}\sqrt{1 + \frac{4\alpha(\alpha-1)(1-\theta)}{1+\theta}}, \quad (14)$$

where the value of p has been substituted from (12). Clearly, the saturation value of the tanh-type boundary-layer solution as $\tilde{x} \to \infty$ depends on α.

(ii) If $1 - \beta < \rho_{\rm out,-}(x = 1)$, then a boundary-layer solution of negative slope is expected (as in Fig. 3).

In this case, a coth-type boundary layer is expected to satisfy the boundary condition at $x = 1$. Various constants of the solution in this case can be found out in the same way as done for the tanh boundary layers.

B. Coexistence line

The coexistence line can be approached from the low-density phase by lowering the value of β, keeping α fixed. As we have seen above [Eq. (14)], in the low-density phase, the saturation value of the tanh-type boundary layer as $\tilde{x} \to \infty$ depends on α. Further, this saturation happens beyond the physical size of the system (i.e., beyond $x = 1$). Thus in the low-density phase, as we lower β, the tanh boundary layer saturates much nearer to the $x = 1$ boundary than earlier. Consequently, the height of the boundary layer increases. For a given α, if the value of the right boundary density, $1 - \beta$, is increased beyond the saturation value of the tanh boundary layer, then the boundary layer can no longer satisfy the boundary condition at $x = 1$. In this situation, the tanh boundary layer is deconfined from the boundary and it enters into the

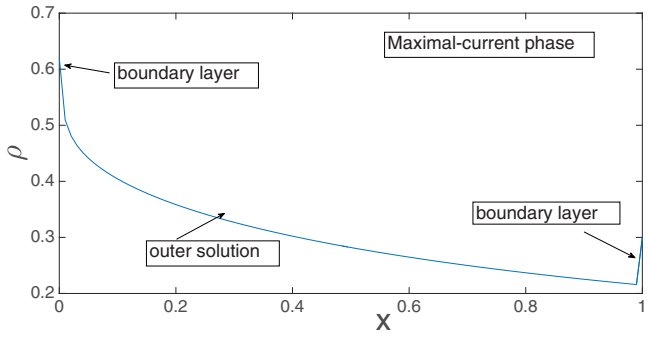

FIG. 4. The density profile in the maximal-current phase with two boundary layers at the two boundaries. There is a boundary layer with negative slope near $x = 0$ boundary. The other boundary layer near $x = 1$ is of tanh type. For this diagram, $\theta = 0.2$.

interior of the system. This condition for deconfinement gives us the condition for coexistence. On the coexistence line, the tanh-type boundary layer appears like a shock (domain wall) separating the high-density and the low-density regions of the density profile. From Eq. (14), the condition for deconfinement of the tanh boundary layer can be expressed as

$$\frac{1}{2}+\frac{p}{2}=\frac{1}{2}+\frac{1}{2}\sqrt{1+\frac{4\alpha(\alpha-1)(1-\theta)}{1+\theta}}=1-\beta. \quad (15)$$

Solving this, we have the equation for the coexistence line as

$$(1-\theta)(\alpha^2-\alpha)=(1+\theta)(\beta^2-\beta). \quad (16)$$

As in the case of TASEP with uniform hopping, on the coexistence line, the tanh-type solution (kink) can be anywhere in the interior of the system with uniform probability. This is unlike the situation with TASEP-LK, which has a shock phase in which the low-density and high-density parts of the density profile are separated by a localized shock. In the next section, we use the fixed-point diagram of the boundary-layer differential equation to explain the origin of such similarities and differences between different TASEPs.

C. Maximal-current phase

The phase transition from the low-density to the maximal-current phase happens with the increase in the value of α for given β. In the low-density phase, the outer solution, $\rho_{\text{out},-}$, satisfies the boundary condition at $x = 0$ until α reaches $\alpha = \alpha_c = \frac{1}{2}$ from below. As we shall show through a fixed-point analysis in Sec. IV, if $\alpha > 1/2$ and β, for example, is sufficiently large ($\beta > 1/2$), then the density profile cannot have an outer solution that satisfies the boundary condition at $x = 0$. In this case, the boundary condition at $x = 0$ must be satisfied by a boundary layer which flows to a bifurcation point at density $\rho = \frac{1}{2}$ in the phase portrait (see the discussion in Sec. IV). As Fig. 4 shows, the boundary layer near $x = 0$ satisfies the boundary condition $\rho(x = 0) = \alpha$ as it approaches the bifurcation point, $\rho = 1/2$, in $\tilde{x} \to \infty$ limit. At the bifurcation point, the boundary layer saturates to an outer solution $\rho_{\text{out},-}$. This saturation to $\rho_{\text{out},-}$ happens near $x = 0$ and the saturation condition can be expressed as $\rho_{\text{in}}(\tilde{x} \to \infty) = \rho_{\text{out},-}(x = 0) = 1/2$. The outer solution, $\rho_{\text{out},-}$ extends until $x = 1$ boundary where the boundary condition is satisfied again through a tanh- or coth-type boundary layer depending on the value of β. Using the condition, $\rho_{\text{out},-}(x = 0) = \frac{1}{2}$, we find

$$c=-\frac{1-\theta}{8}. \quad (17)$$

The unknown constants in tanh or coth boundary layers near $x = 1$ can be found out from the conditions $\rho_{\text{in}}(\tilde{x} \to -\infty) = \rho_{\text{out},-}(x = 1)$ and $\rho_{\text{in}}(\tilde{x} = 0) = 1 - \beta$.

D. β-dominated phase or the high-density phase

Let us consider that in the maximal-current phase, the boundary condition at $x = 1$ is satisfied through a tanh boundary layer. For simplicity, we fix the value of α. Now, as the value of β is decreased, the height of the boundary layer increases. This is similar to the approach to the coexistence line from the low-density phase. The tanh-type boundary layer continues to be present until $1 - \beta$ becomes exactly same as the saturation value of the tanh solution. Thus, the condition

$$\frac{1}{2}+\frac{p}{2}=1-\beta \quad (18)$$

leads to the critical value of β. The value of p can be found from the condition of saturation of the boundary-layer solution to the bulk solution in the $\tilde{x} \to -\infty$ limit, i.e., $\rho_{\text{out},-}(x = 1) = \rho_{\text{in}}(\tilde{x} \to -\infty)$. With c as shown in Eq. (17), we have

$$p=\sqrt{\frac{2\theta}{1+\theta}}. \quad (19)$$

Finally, from (18), we find

$$\beta_c=\frac{1}{2}-\frac{1}{2}\sqrt{\frac{2\theta}{1+\theta}}. \quad (20)$$

For $\beta < \beta_c$, the system is in the high-density phase in which the outer solution satisfies the boundary condition at $x = 1$. Further, since $1 - \beta > 1/2$, we expect the outer solution to be described by $\rho_{\text{out},+}$ with $c = \frac{1}{2}\beta(\beta - 1)(1 + \theta)$. It can be seen that $\rho_{\text{out},+} = \frac{1}{2} + \frac{1}{2}\sqrt{1 + \frac{2\beta(\beta-1)(1+\theta)}{\theta(x-1/2)+1/2}}$ is physically acceptable (not imaginary) along the entire range of x if $\beta < \beta_c$. Note that, in the above expression, the second term under the square root has the largest negative value when $x = 0$. The condition of a real value of $\rho_{\text{out},+}$ leads to $\beta_\pm = \frac{1}{2} \pm \frac{1}{2}\sqrt{\frac{2\theta}{1+\theta}}$. β_-, which is same as β_c, corresponds to the boundary between the high-density and maximal-current phase since for $\beta > \beta_c$, the bulk density given by $\rho_{\text{out},+}$ becomes imaginary. β_+ is not relevant here since, for this value of β, the system is expected to be in the maximal-current phase.

The boundary layer, in the high-density phase, appears near the $x = 0$ boundary. Whether the slope of the boundary layer is positive or negative depends on the boundary condition at $x = 0$. If $\alpha > \rho_{\text{out},+}(x = 0)$, then we have a boundary layer of the form $\rho_{\text{in}}(\tilde{x}) = \frac{1}{2} + \frac{p}{2}\coth[p(\tilde{x} + k)]$. As in the low-density case, the integration constants p and k are determined from the boundary condition and the saturation condition that the boundary layer must satisfy. The boundary condition $\rho_{\text{in}}(\tilde{x} = 0) = \alpha$ leads to the equation $p \coth[pk] = 2\alpha - 1$, and the saturation condition $\rho_{\text{in}}(\tilde{x} \to \infty) = \rho_{\text{out},+}(x = 0)$ leads to $p = \sqrt{1 + \frac{4\beta(\beta-1)(1+\theta)}{(1-\theta)}}$. If $\alpha < \rho_{\text{out},+}(x = 0)$, then the boundary

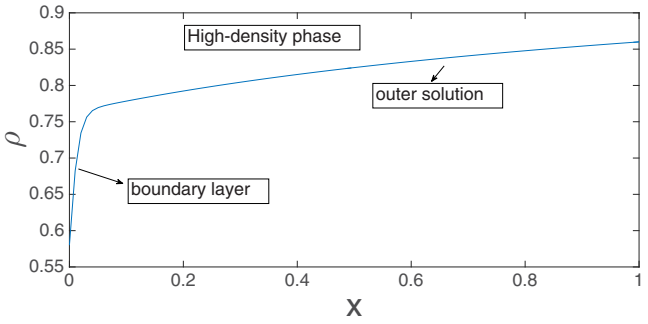

FIG. 5. The density profile in the high-density phase. There is a tanh-type boundary layer near $x = 0$. For this diagram, $\theta = 0.2$.

layer is of the form $\rho_{\rm in} = \frac{1}{2} + \frac{p}{2}\tanh[p(\tilde{x} + k)]$, with p and k determined from similar conditions as described above. A typical density profile in the high-density phase appears as shown in Fig. 5.

IV. FIXED-POINT ANALYSIS OF THE BOUNDARY-LAYER DIFFERENTIAL EQUATION

On one integration, the boundary-layer equation [Eq. (8)] can be written in the form

$$\frac{1}{2}\frac{d\rho}{d\tilde{x}} = c_0 - (\rho^2 - \rho), \tag{21}$$

where c_0 is the integration constant. Since the boundary layer saturates to the outer solution in the appropriate limit, $c_0 = \rho_b(\rho_b - 1)$, where ρ_b denotes the value of the bulk density to which the boundary-layer solution saturates. Clearly, the value of c_0 lies in the range $[-\frac{1}{4} : 0]$. The fixed points (critical points) of Eq. (21) are $\rho^*_{\rm in} = \frac{1}{2}[1 \pm \sqrt{1 + 4c_0}]$. Figure 6 displays the two fixed-point branches as functions of c_0 with a bifurcation point $(c_0, \rho^*_{\rm in}) = (-\frac{1}{4}, \frac{1}{2})$. The vertical arrows in this diagram

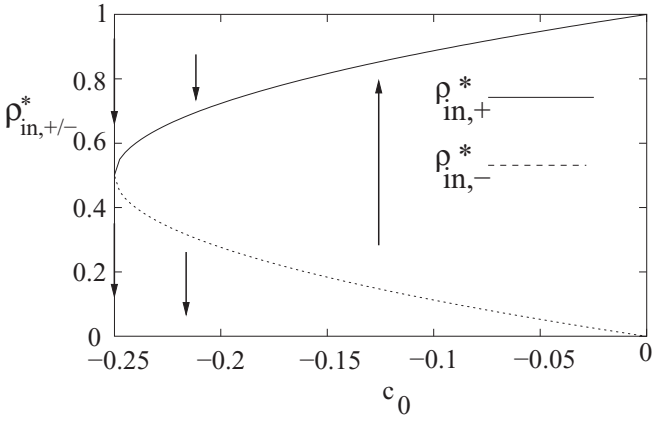

FIG. 6. The fixed-point diagram of the boundary-layer differential equation. The curves in solid and dashed lines indicate the two fixed-point branches. The vertical arrows indicate that the upper and lower fixed-point branches are, respectively, stable and unstable. Thus, these arrows indicate the direction of the flow of the boundary-layer solution as $\tilde{x}$ increases. The point $(-\frac{1}{4}, \frac{1}{2})$ corresponds to the bifurcation point. The flow towards or away from this special point is indicated through vertical downward arrows on the y axis.

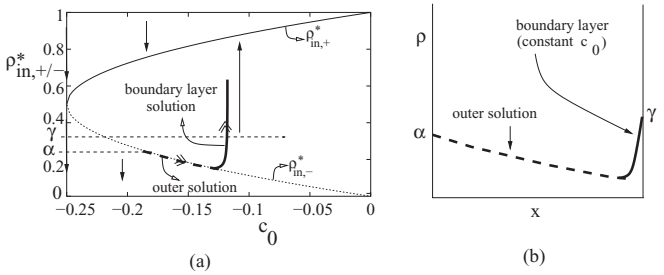

FIG. 7. (a) A typical density profile in the low-density phase is shown on the fixed-point diagram for the boundary-layer equation [Eq. (21)]. The density profile is indicated through the bold (dashed and solid) line with double arrows. The double arrow indicates the direction of increasing x. The vertical, bold solid line indicates the boundary-layer part of the profile. This part is governed by Eq. (21) with constant c_0. The boundary-layer part of the solution satisfies the boundary condition $\rho(x = 1) = 1 - \beta = \gamma$ before reaching the stable (upper) fixed-point branch. The bold dashed line indicates the outer solution described by $\rho_{\rm out,-}$. $\rho_{\rm out,-}$ has a negative slope with x. For convenience of the reader, the boundary densities α and γ are marked through horizontal dashed lines on this figure. The other details of the fixed-point diagram are already indicated in Fig. 6. (b) A qualitative plot for the same density profile as a function of x. As in panel (a), the outer solution and the boundary layer are shown in bold-dashed and bold-solid lines, respectively.

indicate the stability properties of the fixed points or in other words, approach (or departure) of any boundary-layer solution to (or from) the fixed-point branches as $\tilde{x} \to \infty$. For different boundary conditions, the shape and the location of the boundary layer may change but the boundary-layer solutions must be consistent with what is predicted by the fixed-point diagram. Below, we show three examples on predictions of the shape of the density profile in the low-density, high-density, and maximal-current phases.

A. Low-density phase

In the low-density phase, the density profile typically appears as presented in Fig. 7. Such density profile appears for $\alpha < 1/2$. The outer solution satisfies the boundary conditions at $x = 0$. Such an outer solution is described by $\rho_{\rm out,-}$ and has a negative slope as shown through the smoothly varying dashed bold line along the lower fixed-point branch. Such an outer solution, if extended up to $x = 1$, does not in general satisfy the boundary condition. If $\rho_{\rm out,-}(x = 1) < 1 - \beta$, then a tanh-type boundary-layer solution appears near $x = 1$. The boundary-layer solution is the solution of Eq. (21) and corresponds to constant c_0. As the figure shows, in the present case the solution approaches the stable fixed-point branch (the upper branch). In terms of the explicit tanh form of the solution, such saturation corresponds to the saturation of the tanh function for large value of its argument. Thus, the boundary-layer solution is consistent with the flow lines approaching the upper (stable) fixed-point branch from the lower (unstable) fixed-point branch. In the low-density phase, the saturation to the stable fixed point happens beyond the boundary at $x = 1$. The boundary layer while approaching the stable, upper fixed-point branch satisfies the boundary condition at $x = 1$ (see also Fig. 2). For β values

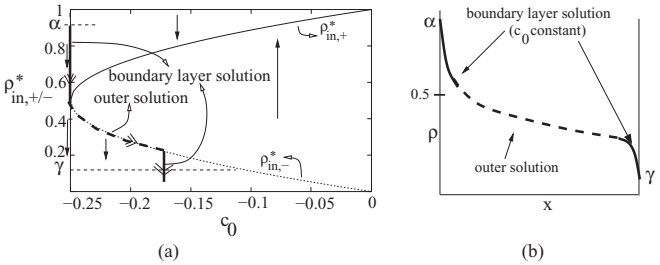

FIG. 8. (a) A typical density profile in the maximal-current phase is shown on the fixed-point diagram for the boundary-layer equation [Eq. (21)]. The density profile is indicated through the bold (dashed and solid) line with double arrows. The double arrows indicate the direction of increasing x. The vertical parts in the bold solid line represent the boundary layers which are governed by Eq. (21) with constant c_0. The boundary-layer part near $x = 0$, represented by a bold line with a double arrow along the y axis, approaches the bifurcation point, $(c_0 = -1/4, \rho = 1/2)$. This boundary layer satisfies the boundary condition at $x = 0$ as it approaches the bifurcation point. The bold-dashed line indicates the outer solution described by $\rho_{\text{out},-}$. $\rho_{\text{out},-}$ has a negative slope with x. The boundary densities, α and γ are marked through horizontal dashed lines on this figure. The other details of the fixed-point diagram are already indicated in Fig. 6. (b) A qualitative plot of the same density profile as a function x. As in panel (a), the outer solution and the boundary layers are shown in bold dashed and bold solid lines, respectively. As shown in panel (a), both the boundary layers have negative slope with x.

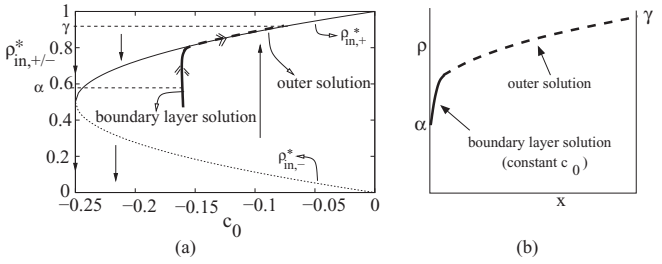

FIG. 9. A typical density profile in the high-density phase is shown on the fixed-point diagram for the boundary-layer equation [Eq. (21)]. The density profile solution is shown through the bold (solid and dashed) line with double arrows. The vertical part in the bold solid line represents the boundary layer of positive slope with x. This part is governed by Eq. (21) with constant c_0. The boundary layer satisfies the boundary condition at $x = 0$. The outer solution shown in the bold dashed line is given by $\rho_{\text{out},+}$. This solution has a positive slope with x. The remaining details of the fixed-point diagram are already indicated in Figs. 6, 7, and 8. (b) A qualitative plot of the same density profile as a function x. As in panel (a), the outer solution and the boundary layers are shown in bold dashed and bold solid lines, respectively. The outer solution has positive slope with x.

for which $\rho_{\text{out},-}(x = 1) > 1 - \beta$, there must be a negative-slope boundary layer described by a coth-type solution. This is consistent with the flow behavior shown through the downward vertical lines below the lower fixed-point branch.

B. Maximal-current phase

For the maximal-current phase, the solution for the density profile has been displayed on the fixed-point diagram of Fig. 8(a). Such a situation occurs when $\alpha > 1/2$ and $\beta > \beta_c$. Let us consider for simplicity $\beta > 1/2$ [i.e., $\rho(x = 1) = 1 - \beta < 1/2$]. Given that $\rho_{\text{out},+}$ has a positive slope with x and the upper fixed-point branch is a stable branch, the only way, the density profile, in this case, can satisfy both the boundary conditions is through boundary layers both at $x = 0$ and $x = 1$. The boundary layer at $x = 0$ has a negative slope with x. It satisfies the boundary condition at $x = 0$ as it approaches the bifurcation point at $\rho = 1/2$ [31]. On the fixed-point diagram, such a boundary layer is represented by the downward line approaching the bifurcation point along the y axis (the solid bold line with double arrows along the y axis). Such a boundary layer is consistent with the downward flow along the y axis shown in Fig. 6. This boundary layer saturates to a smoothly varying outer solution near $x = 0$. The outer solution must be given by $\rho_{\text{out},-}$ since with the positive-slope outer solution, $\rho_{\text{out},+}$, the boundary condition at $x = 1$ cannot be satisfied. The outer solution extends up to the $x = 1$ boundary where the boundary condition is satisfied by a boundary layer. This boundary layer can have upward (described by the tanh solution) or a downward slope (described by a coth solution) depending on whether $\rho_{\text{out},-}(x = 1) < 1 - \beta$ or $\rho_{\text{out},-}(x = 1) > 1 - \beta$, respectively. Both these boundary-layer solutions are consistent with the flow behavior representing flow away from the unstable, lower fixed-point branch. Figure 8(b) shows the density profile plot along x. This type of density profile continues to be present for all $\beta > \beta_c$ and $\alpha > 1/2$.

C. High-density phase

In the high-density phase, $\beta < \beta_c$, the outer solution satisfies the boundary condition at $x = 1$. Such an outer solution is described by $\rho_{\text{out},+}$ and has a positive slope. The boundary condition at $x = 0$ is taken care by a boundary layer of either positive (tanh type) or negative slope (coth-type) solution. While the tanh-type boundary layer is represented by the vertical solid bold line approaching the stable fixed-point branch from below see Fig. 9(a), the coth can be represented in a similar way by a vertical line approaching the stable branch from above. The density profile with a tanh-type boundary layer has been plotted as a function of x in Fig. 9(b).

D. Coexistence line

The coexistence line can be approached from the high- or low-density phases. As we have discussed in Sec. III B, if we approach the coexistence line from the low-density phase by decreasing β for a given α, then the height of the boundary layer near $x = 1$ increases until the saturation value of the tanh-type boundary layer exactly matches with the boundary condition $\rho(x = 1) = 1 - \beta$. At this point, the vertical line in Fig. 7, exactly reaches the upper fixed-point branch right at the $x = 1$ boundary. This condition is expressed in Eq. 15. The vertical line, representing the tanh boundary layer, always approaches the upper fixed-point branch. However, in the low-density phase, the saturation to the upper fixed-point branch happens beyond the physical boundary of the system (i.e., at $x > 1$). It is only at the coexistence line where the saturation happens right at the boundary of the system.

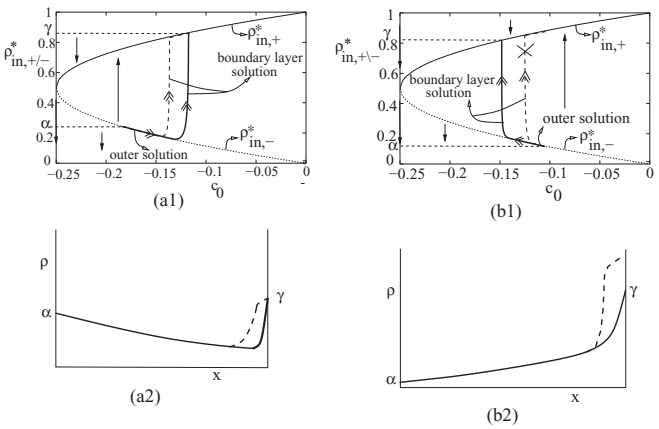

FIG. 10. Diagrams showing the deconfinement of the tanh boundary layer for the present model (a) and for TASEP-LK (b). The outer solutions in panel (a) and panel (b) have slopes of opposite signs. (a1) The boundary layer, just deconfined, has a flexible location. The solid bold line and the dashed bold line with double arrows indicate two possible density profile solutions. Both the density profiles satisfy the given boundary conditions although, for the dashed line, the boundary layer appears in the interior of the system (away from the $x = 1$ boundary) and an outer solution satisfies the boundary condition at $x = 1$. (a2) A qualitative plot for the density profiles of (a1) as functions of x. (b1) The density profile in the solid bold line shows the just-deconfined boundary layer. The dashed-bold line cannot be a solution for the density profile (indicated by a cross mark) since it does not satisfy the boundary condition $\rho(x = 1) = \gamma$ at the $x = 1$ boundary. (b2) A qualitative plot for the density profiles of (b1) as functions of x.

In case of TASEP with uniform hopping, in the low- (high-)density phase, the bulk part of the density profile is constant at a value α $(1 - \beta)$. The boundary layers in low- and high-density phases satisfy the boundary conditions at $x = 1$ and $x = 0$, respectively. As it is here, in both these phases, the boundary layers are described by tanh-type solutions with saturation to $1 - \beta$ (α) for $\tilde{x} \to \infty(\tilde{x} \to -\infty)$ in low- (high-) density phases. The condition for coexistence is same as the present model, except for the fact that for the uniform hopping model the vertical line in the low-density phase saturates to $1 - \beta$ and α at its two ends i.e., for $\tilde{x} \to \infty$ and $\tilde{x} \to -\infty$, respectively. Since the bulk densities (outer solutions) are constant at α and $1 - \beta$, the location of the boundary layer on the coexistence line need not be fixed at a given value of x and, in principle, the boundary layer can be anywhere in the interior of the system with equal probability. A somewhat similar flexibility arises here also since the bulk density has $+ve$ or $-ve$ slope for $\rho > 1/2$ or $\rho < 1/2$, respectively. The shock, thus, joins a gradually decreasing low-density part with a gradually increasing high-density part on its two sides as shown in Fig. 10(a1). The location of the shock along x is flexible since a change in its location only requires a change in the width of the low- or high-density parts and the boundary conditions can still be fulfilled by the low- and high-density regions of the density profile as shown by the two profiles in solid and dashed lines in Figure 10(a1). The density profile in dashed line has the tanh-type boundary layer at a lower value of x than that for the profile in solid line [see also Fig. 10(a2)].

In the following, we compare the properties of shocks that appear in TASEP-LK and in the present model. Briefly, the steady-state density profile of TASEP-LK in the continuum limit is described by a similar equation,

$$\frac{a}{2}\frac{d^2\rho}{dx^2} + (2\rho - 1)\frac{d\rho}{dx} + \Omega(1 - 2\rho) = 0, \tag{22}$$

where a is a small constant proportional to the lattice spacing and the last term proportional to Ω represents the particle adsorption-desorption kinetics on the lattice. Here, we have assumed that particle adsorption or desorption happens at the same rate proportional to Ω. The outer solution (or the bulk solution) which is the solution of the above equation with $a = 0$ is

$$\rho(x) = \Omega x + c, \tag{23}$$

where c is the integration constant. It is straightforward to see that the boundary-layer differential equation for TASEP-LK is same as that in Eq. (8) or (21). Thus, the boundary-layer equation has the same phase portrait as Fig. 6 along with identical boundary-layer solutions as those in Eq. (9). Despite having the same boundary-layer solutions, the shocks in the present model and in TASEP-LK have different properties. Unlike the present model where the shock location along x is flexible on the coexistence line, in case of TASEP-LK, a shock in the density profile is localized at a fixed value of x. The difference with TASEP-LK arises due to the difference in the nature of the outer solution (or the bulk solution). While in the present case, the slope of the outer solution with x is positive or negative if $\rho > 1/2$ and $\rho < 1/2$, respectively, in case of TASEP-LK, the outer solution shown in Eq. (23) has positive slope for the entire range of the density. In the low-density phase, the density profile of TASEP-LK has a tanh-type boundary layer near the $x = 1$ boundary. However, right on deconfinement of the tanh boundary layer, the boundary layer does not have the freedom to change its location towards the interior of the system since such a boundary layer cannot satisfy the boundary condition at $x = 1$ [see Fig. 10(b1) and 10(b2)]. However, the deconfined boundary layer can enter into the interior of the lattice as β is decreased further. This gives rise to a shock phase with the deconfined boundary layer localized in the interior of the lattice TASEP-LK. As we can see from Figs. 10(a1) and 10(a2), due to outer solutions having opposite slopes in the $\rho > 1/2$ and $\rho < 1/2$ regions, right at the deconfinement, the boundary conditions can be appropriately satisfied even if the location of the boundary layer shifts towards the interior of the lattice (located at $x < 1$). Thus, it appears that the slope of the outer solution is crucial for determining whether the system can have a localized shock or not.

V. SUMMARY

In this paper, we study a TASEP with position-dependent hopping rates of particles. The particles, after being injected into the lattice at a given rate, hop to the neighboring forward site obeying the exclusion principle that prohibits double occupancy of a site. On reaching the other end of the lattice, particles are withdrawn at given rates. In this paper, we consider

the case where the hopping rate of a particle changes linearly with the location of the particle on the lattice.

Depending on the values of the boundary rates, in the steady state, TASEP, in general, can exist in various phases where each phase is characterized by the distinct shape of the average particle density profile. The density profiles, in these systems, contain narrow boundary-layer parts whose shape and location differ significantly in various phases. The aim of the present study is to obtain the steady-state particle density profile by directly solving the differential equation for the average particle density under given boundary densities. The differential equation is obtained through a continuum, mean-field approximation of the master equation and it is singular since its highest- (second-) order derivative term has a negligibly small prefactor. Such singular equations are known to have solutions with boundary-layer parts. We use the method of boundary-layer analysis to solve such singular equations. In this scheme, the boundary-layer part and the rest of the density profile are obtained separately by solving the differential equation in different limits. These two parts are then joined through asymptotic matching to obtain the entire density profile. Broadly, the phase diagram of the present model consists of low-density, high-density, and maximal-current phases. We obtain various phase boundaries by analyzing the solution for the density profile under different boundary conditions.

A significant amount of insight regarding the nature of various phases can be obtained from the fixed-point (critical-point) analysis of the differential equation describing the boundary layer. Since the boundary-layer solution must be consistent with the stability properties of the fixed points, it is possible to predict the shape and the location of the boundary layers even in the absence of an explicit solution for the boundary layer.

In this formulation, the maximal-current phase arises as a special phase where the boundary layer at the left boundary ($x = 0$) of the system approaches a bifurcation point located at particle density, $\rho = 1/2$, on the phase portrait of the boundary-layer differential equation. The expressions for the coexistence line [Eq. (16)] and the special boundary densities α_c and β_c differ from the earlier results [15] in a subtle way. These differences originate from the difference in our original assumption regarding the boundary parameters. While in the present work the boundary densities are $\rho(x = 0) = \alpha$ and $\rho(x = 1) = \gamma = 1 - \beta$, in the earlier work, boundary conditions are specified through the boundary injection and withdrawal rates which we denote here as α' and β', respectively. A relation between the two parameter sets can be found by equating currents at the two boundaries for the two cases as $\alpha'(1 - \alpha) = \alpha(1 - \alpha)(1 - \theta)/2$ and $\beta'(1 - \beta) = \beta(1 - \beta)(1 + \theta)/2$.

The fixed-point diagram of the boundary-layer equation is same as that of TASEP with uniform hopping and with or without particle adsorption-desorption kinetics (Langmuir kinetics). Consequently, some of the broad features of the steady-state phase diagram such as the presence of low-density, maximal-current, and high-density phases seem to be the result of same flow properties of the boundary-layer solution in all these models. The details associated with the phase boundaries, however, depend also on the explicit form of the outer solution. For example, in the present problem, the high-density and the low-density phases are separated by a coexistence line. On this line, the tanh-type boundary layer is deconfined from the boundary and it has a uniform probability to be anywhere inside the lattice. Similar deconfinement of the boundary layer happens also in case of TASEP-LK. However, in case of TASEP-LK, the boundary layer does not have similar flexible location on deconfinement. Further, in TASEP-LK, on reducing β, the system enters into a shock phase where the boundary layer enters into the system in the form of a localized shock. The fixed-point-based boundary-layer analysis allows us to understand why such differences arise in these two models. The phase boundaries for the present model differ significantly from those of TASEP with uniform hopping. However, Eqs. (16) and (20) provide the interpolation formula for variation in θ. For example, as θ reduces, the coexistence line approaches the form $\alpha = \beta$, which is found for TASEP with uniform hopping. In a similar way, β_c, separating the high-density and the maximal-current phase approaches $\frac{1}{2}$ as θ is reduced.

For different functional dependence of the hopping rate on x, the outer solution is likely to change significantly. However, qualitatively, this variation might not have significant effect on the narrow boundary-layer regions. As a consequence, we expect the boundary-layer solutions to remain unchanged. Since the shape of the outer solution and its slope crucially depend on the explicit form of the hopping rate, the shape of the phase diagram and the phase boundaries are likely to change significantly. It would be interesting to look at the details of these features for other forms of hopping rates and find out some of the generic features for such systems.

Finally, it appears that a lot of physical insight regarding the phases and phase boundaries can be obtained from the analysis of the phase portrait of the boundary-layer differential equation. Since this method is based on only the knowledge of the fixed points, their stability properties and the slopes of the outer solutions, such methods might be useful for understanding phases and phase transitions in different types complex driven exclusion processes.

ACKNOWLEDGMENTS

Author thanks CSIR-CFTRI for computational facilities and DST, India, for financial support through Grant No. EMR/2016/06266.

[1] D. Mukamel, *Soft and Fragile Matter: Nonequilibrium Dynamics, Metastability and Flow* (IoP Publishing, Bristol, 2000).

[2] J. Krug, Phys. Rev. Lett. **67**, 1882 (1991).

[3] B. Derrida, E. Domany, and D. Mukamel, J. Stat. Phys. **69**, 667 (1992).

[4] M. R. Evans, D. P. Foster, C. Godreche, and D. Mukamel, Phys. Rev. Lett. **74**, 208 (1995); J. Stat. Phys. **80**, 69 (1995).

[5] J. S. Hager, J. Krug, V. Popkov, and G. M. Schütz, Phys. Rev. E **63**, 056110 (2001); V. Popkov, A. Rákos, R. D. Willmann, A. B. Kolomeisky, and G. M. Schütz, *ibid.* **67**, 066117 (2003).

[6] V. Popkov and I. Peschel, Phys. Rev. E **64**, 026126 (2001).
[7] V. Popkov and G. M. Schütz, J. Stat. Phys. **112**, 523 (2003).
[8] R. J. Harris and R. B. Stinchcombe, Physica A **354**, 582 (2005).
[9] M. R. Evans, Y. Kafri, K. E. P. Sugden, and J. Tailleur, J. Stat. Mech. (2011) P06009.
[10] Y.-Q. Wang, R. Jiang, A. B. Kolomeisky, and M.-B. Hu, Sci. Rep. **4**, 5459 (2014).
[11] S. Klumpp and R. Lipowsky, J. Stat. Phys. **113**, 233 (2003).
[12] A. Parmeggiani, T. Franosch, and E. Frey, Phys. Rev. E **70**, 046101 (2004); M. R. Evans, R. Juhász, and L. Santen, *ibid.* **68**, 026117 (2003).
[13] J. Tailleur, M. R. Evans, and Y. Kafri, Phys. Rev. Lett. **102**, 118109 (2009).
[14] A. Melbinger, T. Reichenbach, T. Franosch, and E. Frey, Phys. Rev. E **83**, 031923 (2011).
[15] R. B. Stinchcombe and S. L. A. de Queiroz, Phys. Rev. E **83**, 061113 (2011).
[16] G. Lakatos, T. Chou, and A. Kolomeisky, Phys. Rev. E **71**, 011103 (2005).
[17] G. Lakatos, J. O'Brien, and T. Chou, J. Phys. A **39**, 2253 (2006).
[18] H. Lodish *et al.*, *Molecular Cell Biology*, 5th ed. (W. H. Freeman & Company, New York, 2004).
[19] J. Howard and A. A. Hyman, Curr. Opin. Cell Biol. **19**, 31 (2007).
[20] M. Dogterom *et al.*, J. Cell. Biol. **133**, 125 (1996).
[21] V. Varga *et al.*, Nat. Cell. Biol. **8**, 957 (2006); Cell **138**, 1174 (2009).
[22] M. K. Gardner *et al.*, Cell **135**, 894 (2008).
[23] C. Tischer, D. Brunner, and M. Dogterom, Mol. Syst. Biol. **5**, 250 (2009).
[24] L. Brun *et al.*, Proc. Natl. Acad. Sci. USA **106**, 21173 (2009).
[25] G. Tripathy and M. Barma, Phys. Rev. E **58**, 1911 (1998).
[26] R. J. Harris and R. B. Stinchcombe, Phys. Rev. E **70**, 016108 (2004).
[27] S. L. A. de Queiroz and R. B. Stinchcombe, Phys. Rev. E **78**, 031106 (2008).
[28] S. Mukherji and S. M. Bhattacharjee, J. Phys. A **38**, L285 (2005); S. Mukherji and V. Mishra, Phys. Rev. E **74**, 011116 (2006).
[29] S. Mukherji, Phys. Rev. E **79**, 041140 (2009).
[30] J. D. Cole, *Perturbation Methods in Applied Mathematics* (Blaisdell Publishing, Waltham, MA, 1968).
[31] S. H. Strogatz, *Nonlinear Dynamics and Chaos* (Perseus Books, Cambridge, 1994).